

LETTER OPEN



ACUTE MYELOID LEUKEMIA

The exon-junction complex helicase eIF4A3 holds therapeutic potential in acute myeloid leukemia

Sophia Miliara¹, Elisabetta Cozzi², Xiangfu Zhong¹, Isaac Chan¹, Karl Ekwall¹, Sören Lehmann^{2,3,4}, Andreas Lennartsson¹, Jiri Bartek^{5,6} and Dimitris C. Kanellis⁶

© The Author(s) 2023

Leukemia (2024) 38:663–666; <https://doi.org/10.1038/s41375-023-02098-2>

TO THE EDITOR:

Acute myeloid leukemia (AML) is a diverse hematological cancer characterized by uncontrolled proliferation of myeloid blasts or granulocyte myeloid precursors incapable of terminal differentiation. AML is estimated to represent a low percentage of all newly diagnosed cancer cases but shows increasing incidence and death rates with age [1]. While the causal role and prognostic value of key AML driver mutations have been widely explored [2], the effect of aberrant gene expression or post-transcriptional regulation is less studied, yet equally important. For example, it has been found that alternative splicing of DHX34 induces the expression of nonsense-mediated decay (NMD) products that promote AML [3] and that profiling of gene splicing adds prognostic value to AML-related signatures [4]. Exploration of such avenues may offer new therapeutic approaches since currently a substantial fraction of patients either do not respond, or develop resistance to standard-of-care therapy [5].

eIF4A3 (also known as DDX48), the core RNA helicase of the exon junction complex (EJC), is known to regulate RNA polymerase I and II-associated post-transcriptional events [6]. High expression of eIF4A3 is usually associated with disease progression and poor prognosis in various cancer types [6], which makes it an appealing candidate for cancer therapy. Despite the increasing interest in post-transcriptional mechanisms that affect the onset and progression of AML, eIF4A3 and by extension the EJC has never been previously studied in this context. Here, we provide evidence supporting the dependency of AML on eIF4A3 and we show that high eIF4A3 levels correlate with aberrant expression of genes controlling ribosome biogenesis-associated post-transcriptional mechanisms such as rRNA processing and translation. We further demonstrate that genetic depletion or chemical inhibition of eIF4A3 induces leukemic cell death. Our findings reveal a previously undescribed role for eIF4A3 in AML and suggest eIF4A3 inhibition as a potential therapeutic strategy.

To explore essential genes in AML, we utilized the CRISPR-based knockout screen data included in the DepMap database [7]. We found that across 18 different AML cell lines, the 50 most essential

genes (Supplementary Table S1A) include mainly ribosome proteins (e.g., RPL11, RPS6) and splicing factors (e.g., SNRPE) pointing towards the importance of post-transcriptional mechanisms in AML (Fig. 1A). Indeed, gene ontology analysis of these essential genes showed enrichment in terms covering translation, ribosome biogenesis, splicing, and NMD (Fig. 1B). Notably, such gene list contained an RNA helicase, eIF4A3, that regulates all of the above-mentioned mechanisms and emerges as a candidate therapeutic target in some cancers [6] (Fig. 1A). Importantly, eIF4A3 was the only helicase found in our analysis and showed the highest degree of essentiality among members of the DEAD box family of enzymes (Supplementary Fig. S1A), implicated in the treatment of both solid tumors and blood cancers [8].

To validate such a potentially central role of eIF4A3 in post-transcriptional mechanisms that may propel AML, we then explored the transcriptomic data of DepMap, focusing on the differences between AML cell lines and non-cancerous diploid cells. Firstly, we found that AML cell lines express higher levels of eIF4A3 compared to non-cancerous cells of various lineages (Fig. 1C). This observation was further validated using clinically relevant CD34+ cells from bone marrow-derived samples (two different cohorts: ClinSeq, BEAT-AML [9, 10]) (Fig. 1D, all versus healthy). Given the commonly occurring inter-tumoral heterogeneity of many genes' expression, we next assessed the degree of eIF4A3 variability, allowing us to subdivide the AML cases into three subsets: those expressing low (the bottom 25%), medium (26–75%) or high (top 25%) levels, designated Low, Moderate and High, respectively (Fig. 1D). While the Low subset featured eIF4A3 levels even beyond that seen in healthy controls, both the Moderate and particularly the High subsets showed a robust overexpression of eIF4A3 (Fig. 1D). The widely variable expression of eIF4A3 was also validated with qPCR in RNA samples from a small panel of AML patients (ClinSeq) (Supplementary Fig. 1B).

To explore cellular pathways related to eIF4A3 expression, we then performed a differential expression (DE) analysis and found that 1928 genes were up- and 1531 downregulated (Supplementary Table S1B, C) in the AML subset expressing Low eIF4A3 levels

¹Department of Biosciences and Nutrition, Neo, Karolinska Institute, Huddinge, Sweden. ²Department of Medicine Huddinge, Center for Hematology and Regenerative Medicine, Karolinska Institute, Stockholm, Sweden. ³Department of Medical Sciences, Hematology Unit, Uppsala University, Uppsala, Sweden. ⁴Hematology Centre, Karolinska University Hospital, Stockholm, Sweden. ⁵Danish Cancer Institute, Danish Cancer Society, DK-2100 Copenhagen, Denmark. ⁶Department of Medical Biochemistry and Biophysics, Science for Life Laboratory, Division of Genome Biology, Karolinska Institutet, S-171 21 Stockholm, Sweden. ✉email: jb@cancer.dk; dimitris.kanellis@ki.se

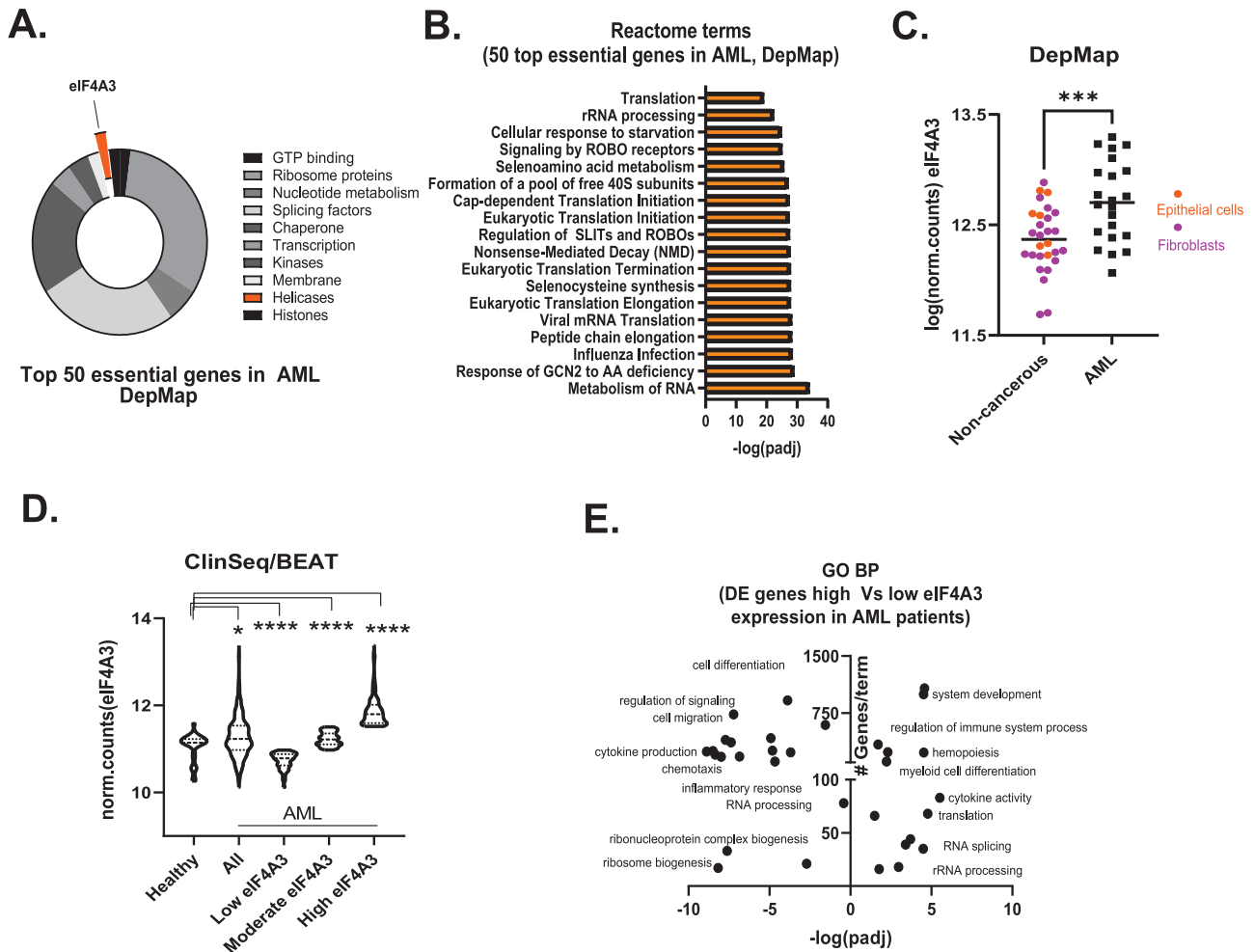


Fig. 1 High expression of eIF4A3 in AML correlates with deregulated post-transcriptional events and ribosome biogenesis. **A** Pie chart showing the categorization of the 50 most essential genes in AML based on their molecular function (DepMap). **B** Barplot of the top Reactome pathway enrichment terms for the top 50 most essential genes in AML. **C** eIF4A3 expression analysis in AML and normal-like (non-cancerous) cell lines. RNA-Seq data were extracted from the DepMap repository. $N = 22$ AML and 28 non-cancerous cell lines, *** $p = 0.01$. **D** eIF4A3 expression in AML and CD34+ bone marrow-derived samples from healthy donors (ClinSeq, BEAT-AML cohorts). AML patients have been sub-grouped based on their eIF4A3 mRNA levels (low: low 25% quartile, high: upper 25% quartile, moderate: second and third quartile, * $p < 0.05$, **** $p < 0.001$). **E** Gene ontology biological process (GO-BP) terms enriched in differentially expressed genes between low and high eIF4A3 expressing AML patients.

compared with High-expressors (identified in Fig. 1D). Such differentially expressed genes showed enrichment in Gene Ontology (GO) terms referring to ribosome biogenesis, translation, and splicing all known to be affected by eIF4A3 (Fig. 1E) [6, 11]. Subsequently, we extended our DE analysis to AML patients versus healthy donors and AML versus non-cancerous cell lines from DepMap (Supplementary Fig. S1C, D and Supplementary Table S1D, E). We found 1871 commonly upregulated and 1214 downregulated genes (Supplementary Table S1F, G) that were then subjected to GO analysis. Again, the upregulated genes belonged to, among other terms, 'rRNA metabolism' and 'translation' (Supplementary Table S1H). Altogether, these results suggest that post-transcriptional mechanisms such as rRNA processing might provide new targets in AML and be explored in future personalized patient profiling to determine sensitivities to relevant pathway inhibitors, possibly including inhibition of eIF4A3 itself.

Indeed, the dependency of AML cells on eIF4A3 suggests that the latter might serve as a therapeutic target. In support of this notion, AML cell lines are more sensitive to CRISPR-mediated eIF4A3 depletion compared to non-cancerous cell lines (DepMap, Supplementary Fig. S2A). Moreover, treatment with an eIF4A3

chemical inhibitor (eIF4A3i, with over 100-fold specificity compared to other eIF4A members or helicases [12, 13]) induced cell death in three different p53^{WT}-carrying AML cell line models (Fig. 2A), a phenotype that could be recapitulated when eIF4A3 was silenced with siRNA (Fig. 2B). Furthermore, healthy donor-originated CD34+ bone marrow cells (Fig. 2C and Supplementary Fig. S2B, C) as well as peripheral blood mononuclear cells (Supplementary Fig. S2D) were less sensitive to eIF4A3 chemical inhibition compared to AML cells further pointing towards a possible therapeutic window.

As p53 was reported to (partially) mediate the effect of eIF4A3 depletion on cell survival [6], we addressed this scenario in AML. Fig. 2B shows that concomitant silencing of eIF4A3 and TP53 reversed partially the effect of eIF4A3 depletion on cell death in two out of three cell lines tested (no response of p53 in OCI-AML2). P53 is the central molecule of the checkpoint induced by impaired ribosome biogenesis (IRBC) [14] that is, a mechanism that is triggered also by eIF4A3 silencing [6]. Focusing on AML, we showed that siRNA-mediated eIF4A3 knock-down induces p53 in an IRBC-mediated fashion since concomitant silencing of RPL5 (a component of the 5S-RNP complex that regulates the IRBC [14]) rescued the effect of eIF4A3 KD on p53 (Fig. 2D).

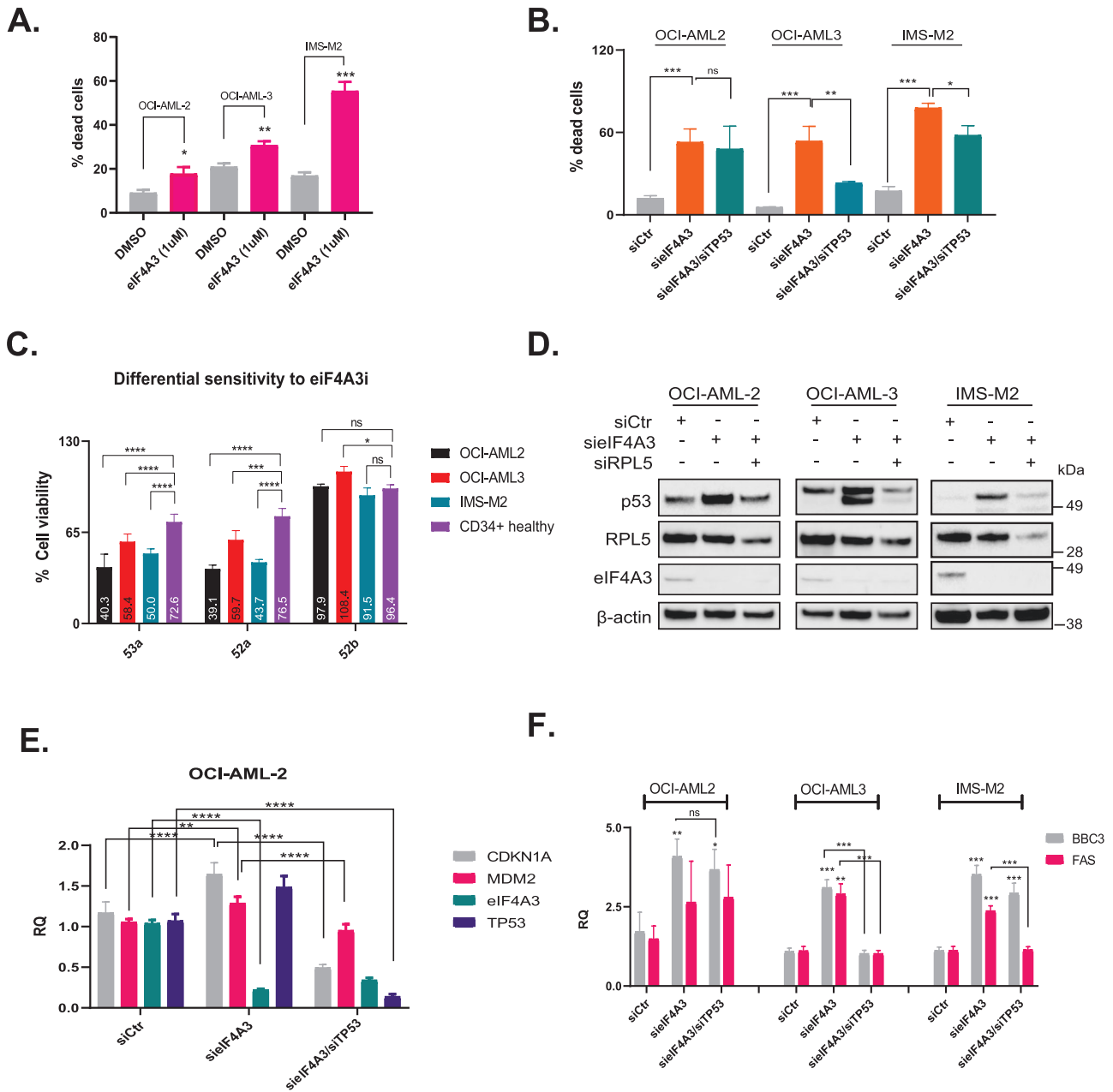


Fig. 2 The eIF4A3/IRBC/p53 axis is essential for AML cell survival. **A** Percentage of OCI-AML-2, OCI-AML-3, or IMS-M2 dead cells in cells treated with the eIF4A3 chemical inhibitor (53a) [13] for 72 h. Data shown as mean \pm SD, $n = 3$ biological replicates, *** $p = 0.01$, ** $p < 0.01$, * $p < 0.05$. **B** Percentage of dead cells following RNAi-mediated silencing of *eIF4A3* for 72 h +/- RNAi-mediated depletion of *TP53*. Data shown as mean \pm SD, $n = 3$ biological replicates, *** $p = 0.01$, ** $p < 0.01$, * $p < 0.05$, ns non-significant. **C** Percentage of viable cells following treatment of AML cells or CD34⁺ bone marrow myeloid cells derived from a healthy donor. Two active eIF4A3 inhibitors (53a, 52a) and one inactive stereoisomer (52b) [13] were used at 4 μ M for 48 h. Data shown as mean \pm SD, $n = 3$ biological replicates, **** $p < 0.001$, *** $p = 0.01$, * $p < 0.05$, ns non-significant. **D** Immunoblotting showing p53, RPL5 and eIF4A3 levels following knock-down of *eIF4A3* +/- *RPL5*. qRT-PCR analysis of *CDKN1A*, *MDM2*, *eIF4A3*, and *TP53* (**E**) or *BBC3* and *FAS* (**F**) mRNA levels in cells depleted of *eIF4A3* +/- *TP53*. In the absence of designating lines (**F**), the asterisks show the comparison to siCtrl. Data shown as mean \pm SD, $n = 3$ biological replicates, **** $p < 0.001$, *** $p = 0.01$, ** $p < 0.01$, * $p < 0.05$, ns non-significant.

EIF4A3 knock-down led to the activation of p53, shown by the upregulation of its direct targets *CDKN1A* and *MDM2*, an effect that was reversed when *TP53* was simultaneously silenced (Fig. 2E, Supplementary Fig. S2E, F). The activation of the IRBC-p53 axis could explain the cytotoxic effect of eIF4A3 inhibition, at least in p53 proficient cells. Indeed, when we investigated the expression levels of two typical p53 apoptotic targets, *BBC3* (PUMA) and *FAS*, we found that *eIF4A3* silencing induced their expression and this was reversed upon simultaneous silencing of *TP53* (Fig. 2F). Of

note, siEIF4A3-mediated *BBC3* upregulation was not dependent on p53 in OCI-AML2 cells (Fig. 2F). This shows that *eIF4A3* silencing can induce apoptotic genes both in a p53-dependent and -independent manner in agreement with previous findings [6] and helps explain the differential sensitivity of AML cell lines to p53-mediated cell death (shown in Fig. 2B).

In conclusion, our data suggest that AML cells are dependent on eIF4A3 and feature aberrant post-transcriptional gene regulation (affecting ribosome biogenesis and other processes),

a vulnerability that could be exploited in AML therapy. To this end, we show that eIF4A3 silencing triggers the IRBC and leads to p53 activation and cell death. Our data show also that siRNA-mediated *eIF4A3* depletion drives cell death even in a p53-independent manner, thereby further expanding the therapeutic potential of eIF4A3 inhibition in AML with mutant p53. We hope that our present data may inspire further preclinical and clinical work, including assessment of in vivo feasibility, and search for predictive biomarkers, to identify AML patients who might most benefit from possible therapeutic targeting of eIF4A3 in the future.

DATA AVAILABILITY

All data generated or analyzed during this study are included in this published article and its supplementary information files. The RNA-Seq data were extracted from either the DepMap consortium or the ClinSeq-AML and BEAT-AML cohorts. Any requests for access to ClinSeq-AML data should be made to SL.

REFERENCES

- Newell LF, Cook RJ. Advances in acute myeloid leukemia. *BMJ*. 2021;375:1–20.
- Kishtagari A, Levine RL, Viny AD. Driver mutations in acute myeloid leukemia. *Curr Opin. Hematol*. 2020;27:49–57.
- Rivera OD, Mallory MJ, Quesnel-Vallières M, Chatrikhi R, Schultz DC, Carroll M, et al. Alternative splicing redefines landscape of commonly mutated genes in acute myeloid leukemia. *Proc. Natl. Acad. Sci. USA* 2021;118:1–10.
- Anande G, Deshpande NP, Mareschal S, Batcha AMN, Hampton HR, Herold T, et al. RNA splicing alterations induce a cellular stress response associated with poor prognosis in acute myeloid leukemia. *Clin Cancer Res*. 2020;26:3597–607.
- van Gils N, Denkers F, Smit L. Escape from treatment; the different faces of leukemic stem cells and therapy resistance in acute myeloid leukemia. *Front Oncol*. 2021;11:1–19.
- Kanellis DC, Espinoza JA, Zisi A, Sakkas E, Bartkova J, Katsori AM, et al. The exon-junction complex helicase eIF4A3 controls cell fate via coordinated regulation of ribosome biogenesis and translational output. *Sci Adv*. 2021;7:1–19.
- Tsherniak A, Vazquez F, Montgomery PG, Weir BA, Kryukov G, Cowley GS, et al. Defining a cancer dependency map. *Cell*. 2017;170:564–76.e16.
- Arna AB, Patel H, Singh RS, Vizeacoumar FS, Kuslik A, Freywald A, et al. Synthetic lethal interactions of DEAD/H-box helicases as targets for cancer therapy. *Front Oncol*. 2023;12:1–14.
- Wang M, Lindberg J, Klevebring D, Nilsson C, Mer AS, Rantalainen M, et al. Validation of risk stratification models in acute myeloid leukemia using sequencing-based molecular profiling. *Leukemia*. 2017;31:2029–36.
- Tyner JW, Tognon CE, Bottomly D, Wilmot B, Kurtz SE, Savage SL, et al. Functional genomic landscape of acute myeloid leukaemia. *Nature*. 2018;562:526–31.
- Le Hir H, Saulière J, Wang Z. The exon junction complex as a node of post-transcriptional networks. *Nat Rev Mol Cell Biol*. 2016;17:41–54.
- Iwatani-Yoshihara M, Ito M, Ishibashi Y, Oki H, Tanaka T, Morishita D, et al. Discovery and characterization of a eukaryotic initiation factor 4A-3-selective inhibitor that suppresses nonsense-mediated mRNA decay. *ACS Chem Biol*. 2017;12:1760–8.
- Ito M, Tanaka T, Cary DR, Iwatani-Yoshihara M, Kamada Y, Kawamoto T, et al. Discovery of Novel 1,4-Diacylpiperazines as Selective and Cell-Active eIF4A3 Inhibitors. *J Med Chem*. 2017;60:3335–51.
- Zisi A, Bartek J, Lindström MS. Targeting ribosome biogenesis in cancer: lessons learned and way forward. *Cancers*. 2022;14:1–29.

AUTHOR CONTRIBUTIONS

Initial conceptualization, SM and DCK; Evolution of conceptualization: all authors; Methodology, SM, EC, XZ, IC and DCK; Formal analysis, SM and DCK; Resources, SL, AL, KE and JB; Data Curation, SM, EC, XZ and DCK; Writing-Review and Editing: all authors; Visualization SM and DCK; Supervision DCK; Funding Acquisition SM, AL and JB. All authors read and approved the final manuscript.

FUNDING

This work was funded by the following grants: the Swedish Cancer Society (grant number: 170176) and the Swedish Research Council (VR-MH 2014-46602-117891-30) (both granted to JB). SM and AL were funded by the Swedish Cancer Society, the Swedish Research Council (VR-MH 2019-01450_3), Radiumhemets forskningsfonder and KI Cancer. KE was funded by the Swedish Cancer Society (grant number 2021/1895) and the Swedish Research Council (grant number 2021-02238). The ClinSeq AML patient RNA-seq data handling (sens2017523 and sens2017533) was supported financially by the Swedish National Infrastructure for Computing (SNIC) at Uppsala Multidisciplinary Center for Advanced Computational Science (UPPMAX) and partially funded by the Swedish Research Council (grant number no. 2018-05973). IMS-M2 cells were kindly provided by Prof. B.Falini. The authors further acknowledge the valuable technical assistance of Louise Lidemalm. Open access funding provided by Karolinska Institute.

COMPETING INTERESTS

The authors declare no competing interests.

ADDITIONAL INFORMATION

Supplementary information The online version contains supplementary material available at <https://doi.org/10.1038/s41375-023-02098-2>.

Correspondence and requests for materials should be addressed to Jiri Bartek or Dimitris C. Kanellis.

Reprints and permission information is available at <http://www.nature.com/reprints>

Publisher's note Springer Nature remains neutral with regard to jurisdictional claims in published maps and institutional affiliations.



Open Access This article is licensed under a Creative Commons Attribution 4.0 International License, which permits use, sharing, adaptation, distribution and reproduction in any medium or format, as long as you give appropriate credit to the original author(s) and the source, provide a link to the Creative Commons licence, and indicate if changes were made. The images or other third party material in this article are included in the article's Creative Commons licence, unless indicated otherwise in a credit line to the material. If material is not included in the article's Creative Commons licence and your intended use is not permitted by statutory regulation or exceeds the permitted use, you will need to obtain permission directly from the copyright holder. To view a copy of this licence, visit <http://creativecommons.org/licenses/by/4.0/>.

© The Author(s) 2023